Applicability of Two-Step Models in Estimating Nitrification Kinetics from Batch Respirograms Under Different Relative Dynamics of Ammonia and Nitrite Oxidation

Kartik Chandran,[1] Barth F. Smets[1,2]

[1]Environmental Engineering Program, University of Connecticut, 261 Glenbrook Road, Storrs, Connecticut 06269-2037. telephone: 860-486-2270, e-mail: barth.smets@uconn.edu
[2]Department of Civil & Environmental Engineering, University of Connecticut, Storrs, Connecticut

Received 17 September 1999; accepted 30 April 2000

Abstract: A mechanistically based nitrification model was formulated to facilitate determination of both NH_4^+-N to NO_2^--N and NO_2^--N to NO_3^--N oxidation kinetics from a single NH_4^+-N to NO_3^--N batch-oxidation profile by explicitly considering the kinetics of each oxidation step. The developed model incorporated a novel convention for expressing the concentrations of nitrogen species in terms of their nitrogenous oxygen demand (NOD). Stoichiometric coefficients relating nitrogen removal, oxygen uptake, and biomass synthesis were derived from an electron-balanced equation.

A parameter identifiability analysis of the developed two-step model revealed a decrease in correlation and an increase in the precision of the kinetic parameter estimates when NO_2^--N oxidation kinetics became increasingly rate-limiting. These findings demonstrate that two-step models describe nitrification kinetics adequately only when NH_4^+-N to NO_3^--N oxidation profiles contain sufficient information pertaining to both nitrification steps. Thus, the rate-determining step in overall nitrification must be identified before applying conventionally used models to describe batch nitrification respirograms.
 Biotechnol Bioeng **70**: 54–64, 2000.
Keywords: nitrification; biokinetics; extant respirometry; two-step model; parameter identifiability

INTRODUCTION

Nitrification involves the sequential oxidation of ammonium-nitrogen (NH_4^+-N, N(-III)) to nitrite-nitrogen (NO_2^--N, N(+III)) and nitrate-nitrogen (NO_3^--N, N(+V)) by two distinct bacterial groups. The stoichiometry of these reactions is described by the following Mole-balanced equations (adapted from Grady et al., 1999).

$$55NH_4^+ + 76O_2 + 109HCO_3^- \rightarrow C_5H_7NO_2 + 54NO_2^- + 57H_2O + 104H_2CO_3 \quad (1)$$

Correspondence to: B. F. Smets

$$400NO_2^- + NH_4^+ + 195O_2 + 4H_2CO_3 + HCO_3^- \rightarrow C_5H_7NO_2 + 3H_2O + 400NO_3^- \quad (2)$$

Though many bacterial genera can perform nitrification, we collectively represent NH_4^+-N oxidizing bacteria using the subscript *ns* and NO_2^--N oxidizing bacteria, by the subscript *nb*, for brevity.

Traditionally, NH_4^+-N to NO_3^--N oxidation has been described as one composite biochemical process using single-step nitrification models that assume NH_4^+-N to NO_2^--N oxidation to be the sole rate-limiting step throughout the oxidation sequence (Grady et al., 1999). Consequently, single-step models are not valid when both NH_4^+-N to NO_2^--N and NO_2^--N to NO_3^--N oxidation limit overall nitrification because they do not consider the dynamics of NO_2^--N oxidation. Two-step models expressed in terms of nitrogen species (Gee et al., 1990; Knowles et al., 1965; Mauret et al., 1996), or oxygen uptake measurements (Brouwer et al., 1998; Ossenbruggen et al., 1996; Ossenbruggen et al., 1991) have been used to estimate kinetic parameters under dual-rate limitation of nitrification by NH_4^+-N and NO_2^--N oxidation. However, in some of these formulations, biochemical phenomena involved in the overall nitrification process are depicted by expressions that do not portray the electron-flow coupling between NH_4^+-N and NO_2^--N oxidation accurately (Ossenbruggen et al., 1996; Ossenbruggen et al., 1991). On the other hand, some two-step models fail to account for NH_4^+-N assimilation by NH_4^+-N oxidizing bacteria (Gee et al., 1990; Knowles et al., 1965; Mauret et al., 1996).

In this study, a two-step nitrification model expressed solely in terms of oxygen-uptake data was derived and used to describe batch NH_4^+-N to NO_3^--N oxidation respirograms obtained with a continuously cultivated highly enriched nitrifying culture.

The specific objectives of this study were:

1. To develop a mechanistically based mathematical model from an electron-balanced equation that explicitly addresses NH_4^+-N to NO_2^--N and NO_2^--N to NO_3^--N oxidation, for describing oxygen-uptake profiles obtained from batch NH_4^+-N oxidation assays.
2. To evaluate whether the kinetics of both NH_4^+-N to NO_2^--N oxidation and NO_2^--N to NO_3^--N oxidation can be determined from a single batch respirogram for complete NH_4^+-N oxidation by applying the two-step model.
3. To evaluate whether kinetic-parameter estimates obtained from experiments where NH_4^+-N and NO_2^--N oxidation are assayed independently, are consistent with kinetic parameter estimates for each oxidation step obtained from complete NH_4^+-N oxidation assays fit with the two-step model.

MATERIALS AND METHODS

Cultivation of a Nitrifying Enrichment Culture

A nitrifying enrichment consortium was grown and maintained in a sequencing batch reactor (SBR) as described elsewhere (Chandran, 1999). Upon attainment of steady state, mixed liquor was periodically withdrawn from the SBR and used in respirometric tests.

Extant Respirometric Assay for Monitoring Nitrification Activity

The kinetics of NH_4^+-N and NO_2^--N oxidation were measured via extant respirometry using low nitrogen to biomass ratios (typically $2 \cdot 10^{-3}$ mg-N/mg biomass COD). The employed respirometric assay was a modification of the method proposed by Ellis et al. (Chandran, 1999; Ellis et al., 1996). Biomass samples were harvested from the parent nitrifying SBR towards the end of the react cycle by centrifugation at 4000 *g* for 10 min. and resuspension in nitrogen-free mineral medium at pH 7.5, containing sufficient added carbonate alkalinity to offset acidification caused by NH_4^+-N oxidation. Respirometric assays were performed at 25°C in a 100-mL jacketed glass vessel, which was completely filled with mixed liquor withdrawn from the parent SBR and sealed with the insertion of a Clark-type polarographic DO electrode (YSI Model 5331, Yellow Springs, OH). The contents of the respirometric vessel were mixed using a magnetic stir-bar. A decrease in the DO level in the vessel due to substrate oxidation was measured by the DO probe and continuously acquired by a personal computer interfaced to a DO monitor (YSI Model 5300, Yellow Springs, OH) by a multi-channel data acquisition device (LabPC+, National Instruments, Austin, TX). DO profiles were acquired at a user-defined frequency (typically 4 Hz) from two respirometric vessels operated in tandem.

Reagent Solutions

Substrate stock solutions were freshly prepared prior to each set of respirometric assays using laboratory grade ammonium sulfate ($(NH_4)_2SO_4$, Fisher Scientific Co., Fair Lawn, NJ) and sodium nitrite ($NaNO_2$, Sigma Chemical Co., St. Louis, MO). Sodium azide (NaN_3, Fisher Scientific Co.) was used to selectively inhibit NO_2^--N to NO_3^--N oxidation.

Nitrogen Analysis

NH_4^+-N, NO_2^--N, and NO_3^--N were analyzed using an ammonia gas-sensing electrode (HNU Systems, Newton, MA), a modification of the sulfanilic acid-*N*-naphthylethylenediamine addition method (Eaton et al., 1995) and a nitrate ion-specific electrode (Corning Inc., Corning, NY), respectively.

Convention for Expressing State Variables

We introduce a novel approach to track state variables during respirometric nitrification assays by expressing reduced nitrogen species concentrations in terms of the nitrogenous oxygen demand (NOD), computed with respect to an appropriate reference nitrogen species (Chandran and Smets, 2000). When NH_4^+-N to NO_2^--N oxidation is considered, NO_2^--N is the reference species; consequently NH_4^+-N has a NOD of 3.43 mg O_2/mg N and NO_2^--N has a NOD of 0 mg O_2/mg N. When oxidation to NO_3^--N is considered, NO_3^--N is the reference species; consequently, NH_4^+-N has an NOD of 4.57 mg O_2/mg N, NO_2^--N has an NOD of 1.14 mg O_2/mg N and NO_3^--N has an NOD of 0 mg O_2/mg N.

Determination of Biomass Concentrations

Biomass concentrations were measured as total chemical-oxygen demand (tCOD) using commercially available reagents (Hach Chemical Co., Loveland, CO). Because the influent was devoid of soluble COD, we express the NH_4^+-N oxidizing biomass and NO_2^--N oxidizing biomass concentrations as follows (Chandran and Smets, 2000).

$$X_{ns}(\text{COD}) = t\text{COD} \cdot \frac{f_{S,ns}}{f_{S,ns} + \frac{f_{S,nb}}{3}} \tag{3}$$

$$X_{nb}(\text{COD}) = t\text{COD} \cdot \frac{\frac{f_{S,nb}}{3}}{f_{S,ns} + \frac{f_{S,nb}}{3}} \tag{4}$$

where:

X_{ns}: NH_4^+-N oxidizing biomass conc. (mg COD L^{-1})
X_{nb}: NO_2^--N oxidizing biomass conc. (mg COD L^{-1})
$f_{S,ns}$: biomass-yield coefficient for NH_4^+-N to NO_2^--N oxidation (mg X_{ns} COD/mg NH_4^+-NOD oxidized)
$f_{S,nb}$: biomass yield coefficient for NO_2^--N to NO_3^--N oxidation (mg X_{nb} COD/mg NO_2^--NOD oxidized)

The (⅓) term associated with $f_{S,nb}$ in Equations (1) and (2) derives from the fact that 1 mg NH_4^+-NOD is oxidized to ⅓ mg NO_2^--NOD.

Kinetics of NH_4^+-N and NO_2^--N Oxidation Obtained Using the Two-Step Nitrification Model

The differential equations representing nitrogen removal, oxygen uptake, and biomass synthesis have been derived earlier and are summarized here in a matrix format (Table I) (Chandran, 1999). Differential equations for each species can be obtained by multiplying the kinetic term in the last column of Table I with the appropriate stochiometric term in columns 2–5.

Though NH_4^+-N is the preferred assimilative nitrogen source for both the NH_4^+-N and NO_2^--N oxidizing microorganisms, the NH_4^+-N requirement of the NO_2^--N oxidizing bacteria is insignificant in comparison to the total nitrogen processed [1 mg NH_4^+-N/400 mg NO_2^--N oxidized, Eq. (2)]. Thus, NH_4^+-N consumption was considered only due to oxidation and assimilation by NH_4^+-N oxidizing bacteria. The four kinetic parameters describing NH_4^+-N and NO_2^--N oxidation, $\mu_{max,ns}$, $K_{S,ns}$, $\mu_{max,nb}$, and $K_{S,nb}$, were estimated by fitting batch respirograms from *complete* NH_4^+-N oxidation assays to the two-step model.

Kinetics of NH_4^+-N and NO_2^--N Oxidation from Isolated Assays

The two nitrification steps were uncoupled by selectively inhibiting NO_2^--N to NO_3^--N oxidation using 24 m*M* NaN_3 (Chandran, 1999; Ginestet et al., 1998). NH_4^+-N to NO_2^--N and NO_2^--N to NO_3^--N oxidation profiles were obtained from *isolated* assays. The kinetic models used to describe respirograms from isolated NH_4^+-N and NO_2^--N oxidation assays were identical to those representing the corresponding processes in the two-step model.

Data Analysis and Parameter Estimation

Dissolved oxygen (DO) profiles obtained from respirometric assays were time-averaged prior to analysis and corrected for endogenous oxygen uptake before substrate injection and after substrate exhaustion. The differential equations linking biomass growth, substrate consumption and oxygen uptake were simultaneously solved using a fourth-order Runge-Kutta method. The biokinetic parameters describing the appropriate nitrogen oxidation step, μ_{max} and K_S, were estimated by minimizing the sum of the squared errors (SSE) between the solution of the appropriate set of differential equations and the experimental oxygen-uptake data using the SOLVER® utility in MS Excel®. Values for $f_{S,ns}$ and $f_{S,nb}$ were estimated from the difference between the total cumulative oxygen uptake during an isolated respirometric assay and the injected NH_4^+-N concentration.

$$f_{S,ns} = \frac{(S_{nh_o} - OU_{ns,f})}{(S_{nh_o} + (0.3 \cdot OU_{ns,f}))} \tag{5}$$

$$f_{S,nb} = \frac{S_{no2_o} - OU_{nb,f}}{S_{no2_o}} \tag{6}$$

where the term $(0.3 \cdot OU_{ns,f})$ in the denominator of Equation (5) represents assimilated NH_4^+-N that does not change oxidation state, and

S_{nho}: initial NH_4^+-N concentration (mg NOD L^{-1})
S_{no2o}: initial NO_2^--N concentration (mg NOD L^{-1})
$OU_{ns,f}$: total cumulative oxygen uptake accompanying NH_4^+-N to NO_2^--N oxidation (mg O_2 L^{-1})
$OU_{nb,f}$: total cumulative oxygen uptake accompanying NO_2^--N to NO_3^--N oxidation (mg O_2 L^{-1})

Due to correlation between μ_{max} and f_S to Monod-type functions (Dochain et al., 1995), small variations in calculated f_S values result in much higher variations in estimated μ_{max} values. To reduce the error in μ_{max} estimates, an average $f_{S,ns}$ value of 0.084 mg X_{ns} COD/mg NH_4^+-NOD was calculated from the entire set of experiments. Minor adjustments to the S_{nho} values used in subsequent data fitting were made in individual experiments based on Ou_f and $f_{S,ns,avg}$.

$$S'_{nh_o} = OU_{ns,f} \cdot \frac{(1 + (0.3 \cdot f_{S,ns,avg}))}{(1 - f_{S,ns,avg})} \tag{7}$$

where:

S'_{nho}: adjusted initial NH_4^+-N concentration (mg NOD L^{-1})

Table I. Elements of the two-step nitrification model.[a]

Oxidation by ↓	S_{nh}	S_{no2}	Ou_{ns}	Ou_{nb}	X_{ns}	X_{nb}	Rate expression
X_{ns}	$-\frac{(1 + (0.3 \cdot f_{s,ns}))}{f_{S,ns}}$	$+\frac{1}{3 \cdot f_{S,ns}}$	$+\frac{(1 - f_{S,ns})}{f_{S,ns}}$		+1		$\mu_{max,ns} \cdot \frac{X_{ns} \cdot S_{nh}}{K_{S,ns} + S_{nh}}$
X_{nb}		$-\frac{1}{f_{S,nb}}$		$+\frac{(1 - f_{S,nb})}{f_{S,nb}}$		+1	$\mu_{max,nb} \cdot \frac{X_{nb} \cdot S_{no2}}{K_{S,nb} + S_{no2}}$

[a]See Nomenclature for definitions.

$f_{S,ns,avg}$: average $f_{S,ns}$ (mg X_{ns} COD/mg NH_4^+-NOD oxidized to NO_2^--N)

$f_{S,nb}$ could not be evaluated from the NO_2^--N oxidation respirograms because the differences between the injected NO_2^--N concentrations and the total cumulative oxygen uptake were too small to estimate reliably. Therefore, a literature $f_{S,nb}$ value of 0.1 mg X_{nb} COD/NO_2^--NOD oxidized was used (Sharma and Ahlert, 1977) and minor corrections to S_{no2o} values were made in individual experiments [Eq. (8)]:

$$S'_{no2_o} = \frac{OU_{nb,f}}{(1 - f_{S,nb,avg})} \tag{8}$$

where:

S'_{no2o}: adjusted initial NO_2^--N concentration (mg NOD L^{-1})

$f_{S,nb,avg}$: average $f_{S,nb}$ (mg X_{nb} COD/mg NO_2^--NOD oxidized to NO_3^--N)

The maximum specific NH_4^+-N and NO_2^--N oxidation activities were expressed as substrate consumption rates (q_{max}) because q_{max} is not affected by a proportional change in both μ_{max} and f_S [Eqs. (9) and (10)].

$$q_{max,ns} = \mu_{max,ns} \cdot \frac{(1 + 0.3 \cdot f_{S,ns})}{f_{S,ns}} \tag{9}$$

$$q_{max,nb} = \frac{\mu_{max,nb}}{f_{S,nb}} \tag{10}$$

where:

$q_{max,ns}$: maximum specific NH_4^+-N consumption rate (mg NOD mg COD^{-1} h^{-1})

$q_{max,nb}$: maximum specific NO_2^--N consumption rate (mg NOD mg COD^{-1} h^{-1})

Individual parameters were obtained from several months of experimental testing. Variability in the parameter pool was minimized by calculating the inner and outer boundaries for each parameter estimate and discarding extreme outliers from the overall parameter set (Ott, 1993). All statistical comparisons employed *t*-tests (Ott, 1993).

Parameter Identifiability Analysis of the Two-Step Nitrification Model

Identifiability analysis of the two-step model parameters was carried out by computing the Fisher information matrix for experimental scenarios of different relative rates of NH_4^+-N and NO_2^--N oxidation. The Fisher information matrix (F) expresses the information content of experimental data and equals (Ljung, 1987):

$$\mathrm{F} = \sum_{j=1}^{N} \left(\frac{\partial y}{\partial \theta_i}(t_j) \right)^T Q_j \left(\frac{\partial y}{\partial \theta_i}(t_j) \right) \tag{11}$$

where:

y: vector of model predictions at time t_j ($j = 1$ to N); (in this case: DO concentrations)

Q: vector containing weighting coefficients (each set to unity in this work)

θ: vector of model parameter ($i = 1$ to P, in this case 4)

The Fisher information matrix is therefore a P × P matrix with diagonal elements of the form:

$$f_{i,i} = \sum_{j=1}^{N} \left(\frac{\partial y}{\partial \theta_i}(t_j) \right)^2 \tag{12}$$

and off-diagonal elements of the form:

$$f_{i,k} = \sum_{j=1}^{N} \left(\frac{\partial y}{\partial \theta_i}(t_j) \right) \cdot \left(\frac{\partial y}{\partial \theta_k}(t_j) \right) \tag{13}$$

To calculate the elements of F for a given experimental data set, a numerical respirometric profile was generated with one of the four two-step model parameters perturbed a small distance ($\delta\theta_i$, typically 1%) from its optimum estimate, keeping all other parameters at their respective optima. The difference between the respirogram thus obtained and the best-fit respirogram was evaluated at each time point (t_j) to give:

$$\frac{\partial y}{\partial \theta}(t_j) \approx \frac{\Delta y}{\Delta \theta_i}(t_j) \tag{14}$$

This procedure was repeated with small perturbations for all other parameters and the resulting F was calculated with Equations (12) and (13). Linearity of the SSE function in the region of perturbation was confirmed by the equality of $\Sigma_{j=1}^{N}\ \partial y/\partial\theta\ (t_j)$ on either side of the optimal parameter estimate.

The following scalar measures of F were computed using functions available in MATLAB® (The Math Works, Natick, MA): trace of F (tr(F)), trace of inverse of F (tr(F^{-1})), determinant of F (det(F)), minimum eigenvalue of F (λ_{min}(F)) and the ratio of the maximum to the minimum eigenvalue of F [λ_{max} (F)/λ_{min} (F)] (Munack, 1991; Vanrolleghem et al., 1995).

Although the original experimental design was not optimized for parameter estimation in this study, inferences on changes in information content of complete NH_4^+-N oxidation profiles could be drawn based on the trends in scalar measures of F, obtained at different relative NH_4^+-N and NO_2^--N oxidation rates. tr(F) was not considered because it is not a reliable estimator of the information content of experimental data (Goodwin, 1987; Vanrolleghem et al., 1995).

The precision of the two-step model kinetic parameter estimates was determined by calculating their standard error (Robinson, 1985).

$$\mathrm{RMS} = \mathrm{SSE}/(\mathrm{N} - \mathrm{P}) \tag{15}$$

$$\mathrm{SE_i} = (\mathrm{RMS} \cdot \mathrm{x_{i,i}})^{0.5} \tag{16}$$

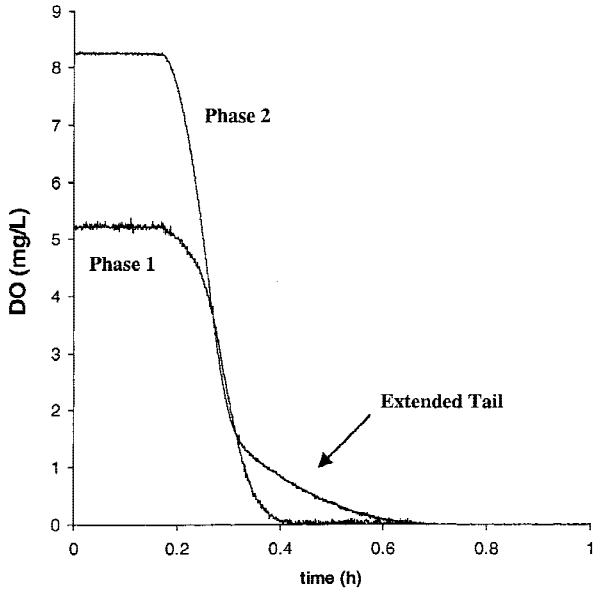

Figure 1. Experimental NH_4^+-N to NO_3^--N oxidation respirograms obtained during phase 1 (NH_4^+-N oxidation rate-limiting, no extended tailing) and phase 2 (Both NH_4^+-N and NO_2^--N oxidation rate-limiting, pronounced extended tailing).

where:

RMS: residual mean square
SE_i: standard error associated with i^{th} parameter

Correlation between the four parameters of the two-step nitrification model was elucidated by plotting *SSE* values as a function of two-parameter combinations normalized against their estimated optima. In addition, the correlation coefficients ρ_{ij} were computed from the covariance matrix (X), which is the inverse of F (Robinson, 1985):

$$\rho_{i,k} = \frac{x_{i,k}}{(x_{i,i} \cdot x_{k,k})^{0.5}} \quad (17)$$

where:

$x_{i,k}$: off-diagonal element of the covariance matrix X
$x_{i,i}$ and $x_{k,k}$: mean diagonal elements of the covariance matrix X

Numerically evaluated sensitivity coefficient profiles, $\theta_i \cdot \partial y/\partial\theta_i(t_j)$ were plotted for all parameters simultaneously to illustrate relative parameter sensitivities (Brouwer et al., 1998).

Partial Inhibition of NO_2^--N Oxidation

In one set of experiments, the kinetics of complete NH_4^+-N oxidation and NO_2^--N oxidation were estimated concurrently, while NO_2^--N oxidation was selectively but partially inhibited by addition of NaN_3 (0.24 and 0.48 μM). The accuracy of the two-step model in quantifying NO_2^--N to NO_3^--N oxidation was ascertained by comparing kinetic parameter estimates obtained from isolated NO_2^--N oxidation assays with those obtained by application of the two-step model to complete NH_4^+-N oxidation profiles.

RESULTS

Temporal Variation in Kinetic Parameter Estimates of NH_4^+-N and NO_2^--N Oxidation from Isolated Assays

The nitrifying SBR was operated for twelve months at a solids retention time (SRT) and hydraulic retention time (HRT) of 20 and 1.25 days, respectively. SBR performance was stable and near complete nitrification was consistently attained (Chandran, 1999).

However, based on the pseudo-first-order rate coefficient, k ($k = q_{max} \cdot X_o/K_s$) calculated from kinetic parameter estimates obtained from isolated respirometric assays, the entire period of study could be divided into two phases. During the first phase, NH_4^+-N oxidation was the sole rate-limiting process ($k_{ns} < k_{nb}$, $\alpha = 0.05$, $df = 36$), while in the second phase, both NH_4^+-N and NO_2^--N oxidation limited overall nitrification ($k_{ns} = k_{nb}$, $\alpha = 0.05$, $\beta = 0.25$, $df = 7$). The temporal shift in the relative kinetics of NH_4^+-N and NO_2^--N oxidation was attributed to a decrease in the

Table II. Two-step model kinetic parameter estimates.

$q_{max,ns}$ mg COD / mg NOD h	$K_{S,ns}$ mg NOD L^{-1}	$q_{max,nb}$ mg COD / mg NOD h	$K_{S,nb}$ mg NOD L^{-1}	Type of cultivation	Source
0.95 ± 0.4	1.54 ± 0.95	1.22 ± 0.78	1.17 ± 0.98	NEC[a]	This study, phase 1
0.74 ± 0.21	0.99 ± 0.36	0.39 ± 0.07	0.41 ± 0.13	NEC	This study, phase 2
(6–14) · 10^{-3}	0.17–0.86	(1.5–3) · 10^{-3}	0.17–0.57	AS[a]	Brouwer et al., 1998
0.19	2.4[b]	0.17	1.14[b]	NEC	Gee et al., 1990
1.42	4.58	1.18	2.51	NEC	Knowles et al., 1965[c]

Note: Conversions from reported values assumed 1.2 mg × COD/mg SS and 1.4 mg × COD/mg VSS.

[a]See Nomenclature for definitions.
[b]Obtained from steady state chemostat data.
[c]Average values.

Table III. Statistical inferences made on kinetic data pool. Parameters (p1 and p2) were compared at a confidence level of 95% ($\alpha = 0.05$) with the null hypothesis; p1 = p2.

Reaction considered in parameter estimation		Assay conducted	Hypothesis on q_{max} (df, α, β)[a]	Hypothesis on K_s (df, α, β)	Hypothesis on k (df, α, β)[b]
NH_4^+–N → NO_2^-–N	from	Complete NH_4^+–N oxidation (Phase 1)	$q_{max,ns,TS} = q_{max,ns}$ (10, 0.05, 0.44)	$K_{S,ns,TS} < K_{S,ns}$ (23, 0.05, –)	$k_{ns,TS} > k_{ns}$ (37, 0.05, –)
	vs				
NH_4^+–N → NO_2^-–N	from	Isolated NH_4^+–N oxidation (Phase 1)			
NO_2^-–N → NO_3^-–N	from	Complete NO_2^-–N oxidation (Phase 1)	$q_{max,nb,TS} > q_{max,nb}$ (31, 0.05, –)	$K_{S,nb,TS} > K_{S,nb}$ (35, 0.05, –)	$k_{nb,TS} > k_{nb}$ (57, 0.05, –)
	vs				
NO_2^-–N → NO_3^-–N	from	Isolated NO_2^-–N oxidation (Phase 1)			
NH_4^+–N → NO_2^-–N	from	Complete NH_4^+–N oxidation (Phase 2)	$q_{max,ns,TS} = q_{max,ns}$ (12, 0.05, 0.21)	$K_{S,ns,TS} < K_{S,ns}$ (4, 0.05, –)	$k_{ns,TS} > k_{ns}$ (21, 0.05, –)
	vs				
NH_4^+–N → NO_2^-–N	from	Isolated NH_4^+–N oxidation (Phase 2)			
NO_2^-–N → NO_3^-–N	from	Complete NO_2^-–N oxidation (Phase 2)	$q_{max,nb,TS} > q_{max,nb}$ (28, 0.05, –)	$K_{S,nb,TS} < K_{S,nb}$ (17, 0.05, –)	$k_{nb,TS} > k_{nb}$ (23, 0.05, –)
	vs				
NO_2^-–N → NO_3^-–N	from	Isolated NO_2^-–N oxidation (Phase 2)			
NH_4^+–N → NO_2^-–N	from	Complete NH_4^+–N oxidation (Phase 1)	$q_{max,ns,1} > q_{max,ns,2}$ (48, 0.05, –)	$K_{S,ns,1} > K_{S,ns,2}$ (43, 0.05, –)	$k_{ns,1} = k_{ns,2}$ (49, 0.05, 0.32)
	vs				
NH_4^+–N → NO_2^-–N	from	Complete NH_4^+–N oxidation (Phase 2)			
NO_2^-–N → NO_3^-–N	from	Complete NH_4^+–N oxidation (Phase 1)	$q_{max,nb,TS1} > q_{max,nbTS2}$ (30, 0.05, –)	$K_{S,nb,TS1} > K_{S,nb,TS2}$ (31, 0.05, –)	$k_{nb,TS1} > k_{nb,TS2}$ (39, 0.05, –)
	vs				
NO_2^-–N → NO_3^-–N	from	Complete NH_4^+–N oxidation (Phase 2)			

Note: See Nomenclature for definitions. Subscripts $_1$ and $_2$ refer to phase 1 and phase 2, respectively.

[a] α: probability of incorrectly rejecting the null hypothesis when it is true. β: probability of incorrectly accepting the null hypothesis when it is false. Only applicable when the null hypothesis is not rejected and the parameters being compared are not significantly different.

[b] K: pseudo-first-order rate coefficient = $(q_{max} \cdot X/K_S)$

NO_2^--N oxidation rate ($k_{nb,phase1} > k_{nb,phase2}$, $\alpha = 0.05$, $df = 32$) because the NH_4^+-N oxidation rate did not change significantly ($k_{ns,phase1} = k_{ns,phase2}$, $\alpha = 0.05$, $\beta = 0.03$, $df = 11$) (Chandran and Smets, 2000).

Kinetics of NH_4^+-N and NO_2^--N Oxidation Using the Two-Step Model

Complete NH_4^+-N oxidation respirograms obtained during the second phase differed from similar respirograms obtained during the first phase, by a singular extended-tailing behavior (Fig. 1). Extant respirometric assays performed with biomass samples that had been exposed to sublethal doses of azide, revealed that progressively lower rates of NO_2^--N oxidation gave rise to an increasingly prominent extended tail, suggesting that the tailing observed in the second phase was caused by slow NO_2^--N oxidation kinetics. The temporal trends in NH_4^+-N and NO_2^--N oxidation predicted from isolated assays were well captured by the two-step model ($k_{ns,TS1} = k_{ns,TS2}$, $k_{nb,TS1} > k_{nb,TS2}$; Tables II and III). However, during both phases, the pseudo-first-order rate coefficients for NH_4^+-N and NO_2^--N oxidation derived from complete NH_4^+-N to NO_3^--N oxidation respirograms were significantly higher than those derived from isolated assays ($k_{ns,TS} > k_{ns}$, $k_{nb,TS} > k_{nb}$; Table III). The significant difference in the kinetic parameter estimates obtained from isolated NH_4^+-N oxidation and NO_2^--N oxida-

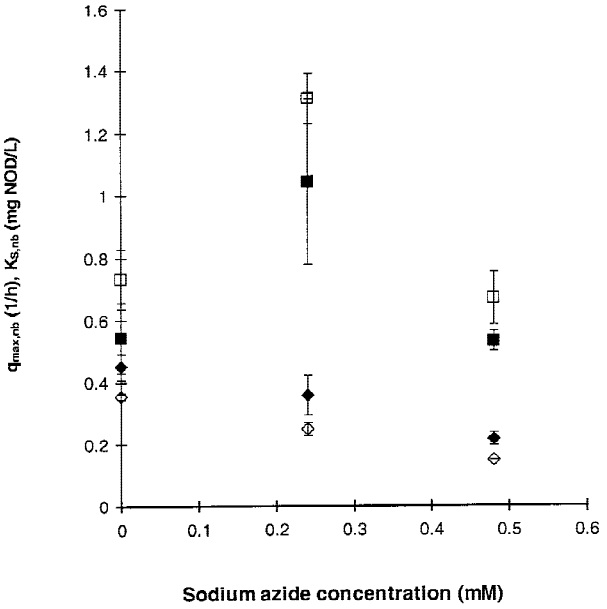

Figure 2. Accuracy of two-step model kinetic parameter estimates $q_{max,nb}$ (◇) and $K_{S,nb}$ (□). The filled symbols represent the parameter estimates obtained from the two-step model fits. The open symbols represent the parameter estimates from isolated assays.

tion assays and complete NH_4^+-N oxidation assays was attributed to the temporal variance of the estimates during the course of this study.

To eliminate the time-dependent variation of the kinetic parameter estimates that compromises statistical comparisons, the kinetics of NO_2^--N oxidation were estimated concurrently from isolated NO_2^--N oxidation assays and by applying the two-step model to a complete NH_4^+-N oxidation respirogram. The estimates for NO_2^--N oxidation obtained from these two methods were in good agreement (Fig. 2). Thus, when nitrification is limited by both NH_4^+-N and NO_2^--N oxidation, the two-step model accurately portrays NO_2^--N oxidation.

Identifiability of the Two-Step Model Parameters

The identifiability of the four parameters in the two-step model was studied with three representative profiles of NH_4^+-N to NO_3^--N oxidation. One profile was tested from phase 1 (case 1) and phase 2 (case 2) and an additional profile was taken from the second phase when NO_2^--N oxidation was further inhibited by NaN_3 addition (0.48 μM, case 3). When NH_4^+-N oxidation was the sole rate-limiting step (case 1), all parameters were strongly correlated as evidenced by long narrow valleys in the SSE-response surfaces for two-parameter combinations (Fig. 3). Additionally, all correlation coefficients were close to unity (Table IV) and sensitivity profiles for all parameters overlapped considerably (Fig. 5). When nitrification was limited by both NH_4^--N and NO_2^--N oxidation (cases 2 and 3), only the ($\mu_{max,ns}$, $K_{S,ns}$) and ($\mu_{max,nb}$, $K_{S,nb}$) parameter combinations were strongly correlated (correlation coefficients > 0.9 (Robinson, 1985; Fig. 4, Table IV) while the correlation in the other four parameter combinations decreased significantly (Table IV). Further, the sensitivity profiles for $\mu_{max,ns}$

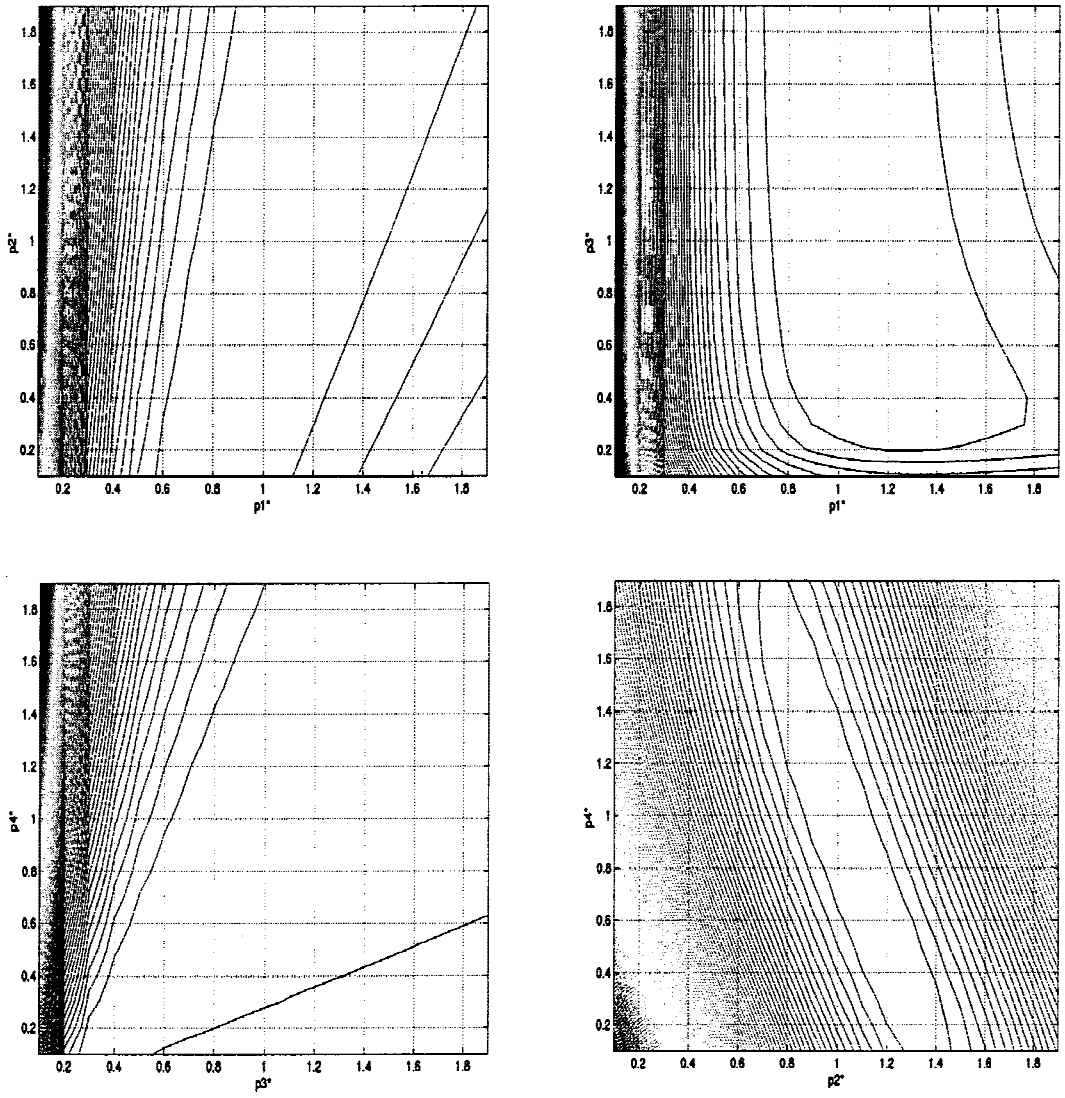

Figure 3. *SSE* response surfaces around best-fit estimates of selected parameter combinations. Case 1 $k_{ns} < k_{nb}$. Initial conditions: $S_{nho} = 7.4$ mg NH_4^+-NOD L^{-1}, $X_{ns} = 274$ mg COD L^{-1}, $X_{nb} = 63$ mg COD L^{-1}. Best fit parameter estimates: $q_{max,ns} = 0.3\ h^{-1}$, $K_{S,ns} = 1.4$ mg NOD L^{-1}, $q_{max,nb} = 2.3\ h^{-1}$, $K_{S,nb} = 1.3$ mg NOD L^{-1}. pl*, p2*, p3*, and p4* denote $\mu_{max,ns}$, $K_{S,ns}$, $\mu_{max,nb}$, and $K_{S,nb}$, respectively, normalized with respect to the best fit parameter estimates.

Table IV. Correlation coefficients between different two-parameter sets of the two-step model.

Case	Rate-limiting oxidation step	Correlation coefficients between $\mu_{max,ns}$ (p1), $K_{S,ns}$(p2), $\mu_{max,nb}$ (p3) and $K_{S,nb}$ (p4)					
		p1–p2	p3–p4	p1–p4	p2–p3	p1–p3	p2–p4
1	NH_4^+–N to NO_2^-–N	0.93	0.99	0.78	0.93	0.81	0.9
2	NH_4^+–N to NO_2^-–N and NH_2^-–N to NO_3^-–N	0.98	0.99	0.54	0.54	0.56	0.54
3	NH_2^-–N to NO_3^-–N (severely)	0.98	0.99	0.2	0.18	0.21	0.16

and $K_{S,ns}$ were clearly distinguishable from those for $\mu_{max,nb}$ and $K_{S,nb}$; NH_4^+-N oxidation kinetics and NO_2^--N oxidation kinetics had the largest impact on the initial and latter part of the oxygen uptake profile, respectively (Fig. 6).

Information Content of Complete NH_4^+-N Oxidation Profiles

The information content of the complete NH_4^+-N oxidation respirogram was evaluated based on computed scalar mea-

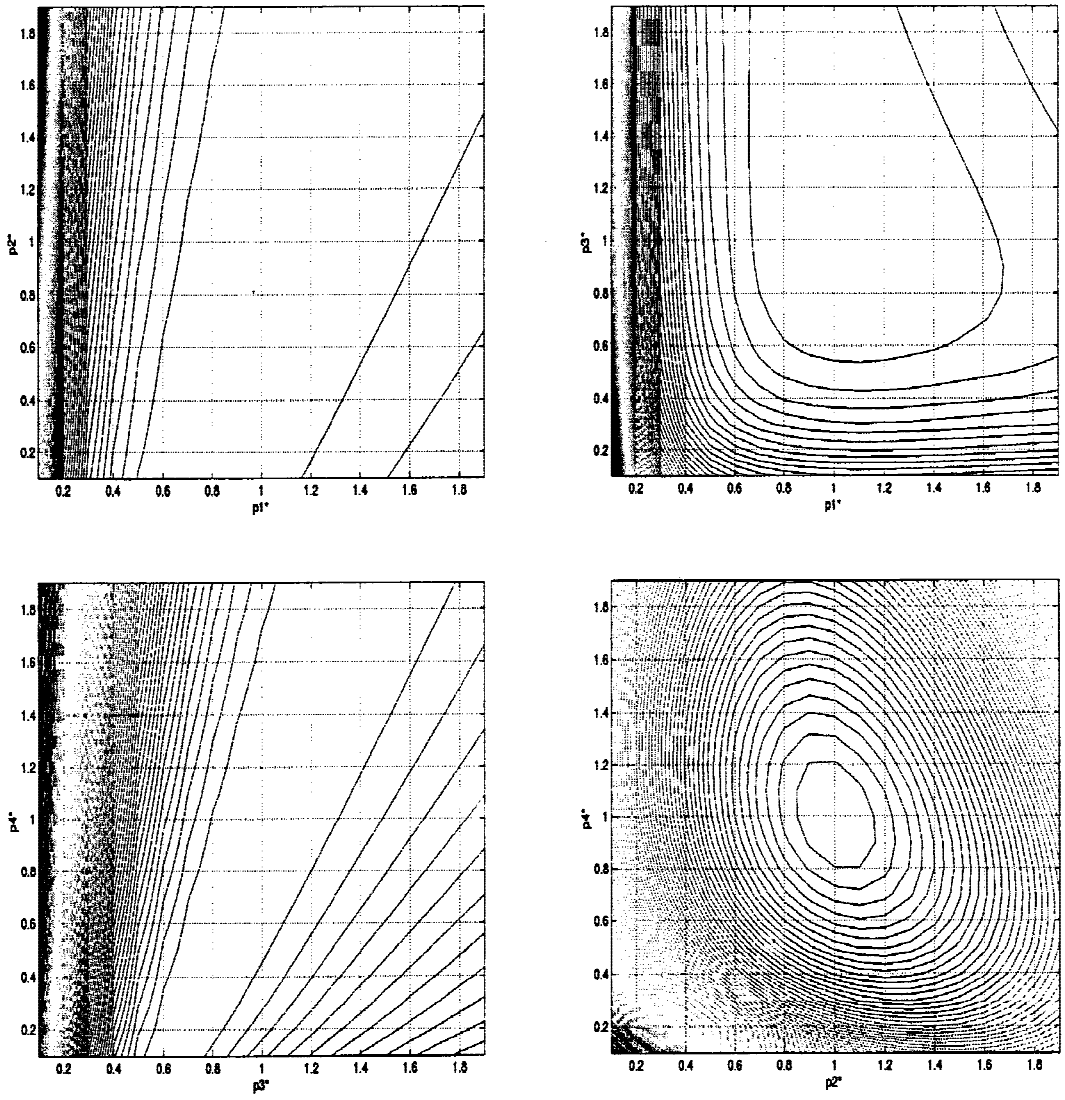

Figure 4. *SSE* response surface around best-fit estimates of selected parameter combinations. NO_2^--N to NO_3^--N oxidation partially inhibited in Case 3, $k_{ns} > k_{nb}$. Initial conditions: S_{nho} = 6.5 mg NH_4^+-NOD L^{-1}, X_{ns} = 431 mg COD L^{-1}, X_{nb} = 163 mg COD L^{-1}. Best fit parameter estimates: $qmax_{ns}$ = 0.3 h^{-1}, $K_{S,ns}$ = 1.6 mg NOD L^{-1}, $q_{max,nb}$ = 0.2 h^{-1}, $K_{S,nb}$ = 0.5 mg NOD L^{-1}. p1*, p2*, p3*, and p4* denote $\mu_{max,ns}$, $K_{S,ns}$, $\mu_{max,nb}$ and $K_{S,nb}$, respectively, normalized with respect to the best fit parameter estimates.

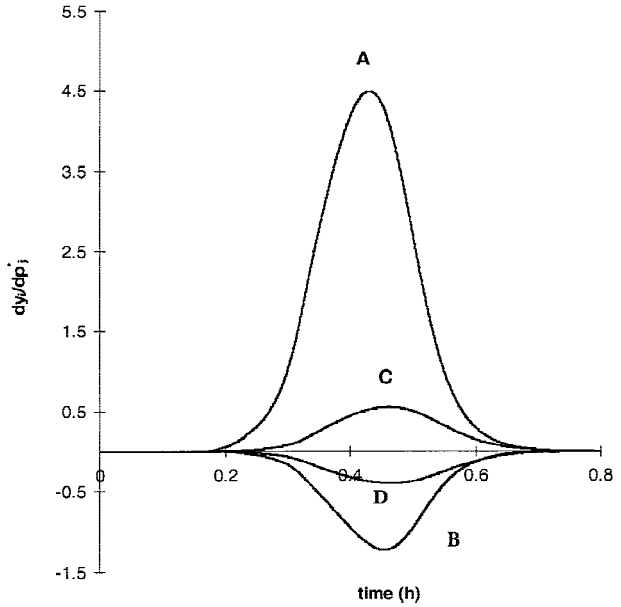

Figure 5. Sensitivity plots corresponding to data fits described in Figure 3. Curves A, B, C, and D represent the sensitivity profiles for $\mu_{max,ns}$, $K_{S,ns}$, $\mu_{max,nb}$ and $K_{S,nb}$, respectively.

sures of the Fisher information matrix (Table V). With progressively slower NO_2^--N oxidation kinetics (case 1 to case 3), values of $\lambda_{min}(F)$ and $det(F)$ monotonically increased and values of $tr(F^{-1})$ monotonically decreased indicating an improvement in the information content of the NH_4^+-N oxidation profile (Table V). In contrast, the values of $\lambda_{max}(F)/\lambda_{min}(F)$ decreased initially (case 1 to case 2) but increased slightly upon a further reduction in NO_2^--N oxidation kinetics (case 2 to case 3).

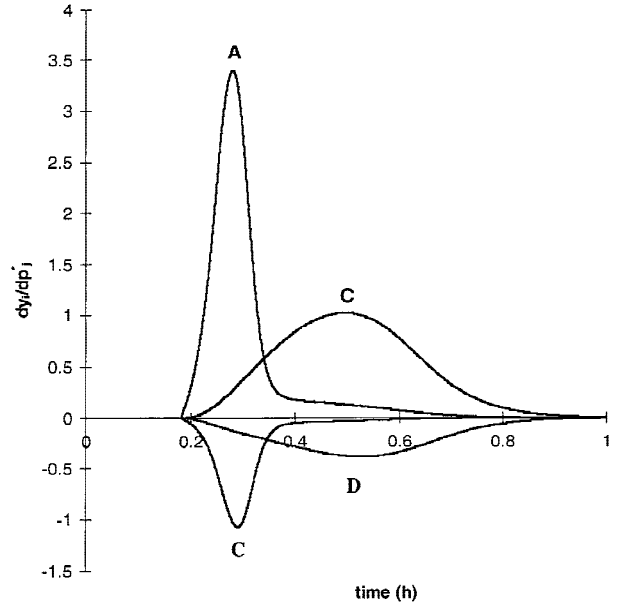

Figure 6. Sensitivity plots corresponding to data fits described in Figure 4. Curves A, B, C, and D represent the sensitivity profiles for $\mu_{max,ns}$, $K_{S,ns}$, $\mu_{max,nb}$, and $K_{s,nb}$, respectively.

Precision of Kinetic Parameter Estimates Using the Two-Step Model

An examination of the standard errors in all two-step model parameter estimates for both oxidation steps revealed a steady increase in precision with slower NO_2^--N oxidation kinetics ($SE_{case1} > SE_{case2} > SE_{case3}$; Table VI). The standard errors for $K_{S,ns}$ and $K_{S,nb}$ were higher than those for $\mu_{max,ns}$ and $\mu_{max,nb}$ for all relative NH_4^+-N and NO_2^--N oxidation dynamics. The improvement in precision of $\mu_{max,nb}$ and $K_{S,nb}$ estimates with a reduction in NO_2^--N oxidation kinetics was higher than that of $\mu_{max,ns}$ and $K_{S,ns}$ estimates. Under severe rate-limitation by NO_2^--N oxidation, the precision of $\mu_{max,nb}$ and $K_{S,nb}$ estimates was higher than that of $\mu_{max,ns}$ and $K_{S,ns}$ estimates.

DISCUSSION

The average kinetic parameters derived from two-step model fits to complete NH_4^+-N oxidation respirograms are in good agreement with those previously reported for enriched nitrifying consortia (Table II). However, the slightly lower values of $K_{S,ns}$ and $K_{S,nb}$ determined in this study indicate the high affinity of the enrichment towards NH_4^+-N or NO_2^--N after continuous cultivation for approximately 12 months with a low-substrate-loading rate and are similar to those from steady-state chemostat data (Gee et al., 1990). The higher K_S values reported by Knowles et al. (1965) (Table II) may also be due to relatively high initial NH_4^+-N concentration of approximately 15 mg NH_4^+-N L^{-1}. In contrast, the maximum concentrations in our assays were near 4 mg NH_4^+-N L^{-1} and 3 mg NO_2^--N L^{-1}, thereby resulting in low K_S estimates. The values of the maximum specific NH_4^+-N and NO_2^--N consumption rates presented in Brouwer et al. (1998; Table II) are anomalously low because these are calculated based on the total suspended solids concentration of an activated sludge instead of the nitrifying biomass concentration (Brouwer et al., 1998).

Available two-step nitrification models are either based on substrate depletion profiles (Gee et al., 1990; Knowles et al., 1965; Mauret et al., 1996) or a combination of substrate- and oxygen-uptake measurements (Ossenbruggen et al., 1996; Ossenbruggen et al., 1991). A recent model (Ossenbruggen et al., 1996) differentiated overall nitrification into a first stage where both NH_4^+-N and NO_2^--N are concomitantly oxidized and a second stage where NH_4^+-N is exhausted but NO_2^--N is still oxidized. During the first stage, concurrent NH_4^+-N and NO_2^--N oxidation was described by a combination of Monod kinetics for NH_4^+-N to NO_3^--N oxidation and a linear term for inhibition by NO_2^--N. NO_2^--N oxidation in the second stage was depicted by a Monod term. Thus, in effect, the "two-step" model (Ossenbruggen et al., 1996) is a single-step model for the first stage. Additionally, the maximum NO_2^--N concentration observed in the study was approximately 5 mg NO_2^--N L^{-1}, which is far lower than the NO_2^--N levels inhibitory to NH_4^+-N oxidation (~1200 mg NO_2^--N L^{-1}) (Prakasam and Loehr, 1972). With our enrichment, NH_4^+-N to NO_2^--N oxidation was not affected by NO_2^--N concentrations as

Table V. Scalar measures of the Fisher information matrix for representative experimental batch NH_4^+−N oxidation profiles.

Case	Rate-limiting oxidation step	$tr(F^{-1})$	$det(F)$	$\lambda_{min}(F)$	$\left[\frac{\lambda_{max}(F)}{\lambda_{min}(F)}\right]$
1	NH_4^+−N to NO_2^-−N	91.68	$1.04 \cdot 10^8$	0.011	$5.11 \cdot 10^8$
2	NH_4^+−N to NO_2^-−N and NH_2^-−N to NO_3^-−N	2.04	$1.03 \cdot 10^{12}$	0.62	$2.97 \cdot 10^6$
3	NH_2^-−N to NO_3^-−N (severely)	0.78	$7.61 \cdot 10^{13}$	1.88	$3.3 \cdot 10^6$

high as 100 mg NO_2^--N L^{-1} (Chandran, 1999). Thus, we believe that the nitrification model proposed by Ossenbruggen et al., (1996) is mechanistically incorrect.

There are very few two-step nitrification models that are based solely upon oxygen-uptake data. NH_4^+-N and NO_2^--N oxidation are explicitly considered in the oxygen-uptake-based model proposed by Brouwer et al. (1998). However, due to equations describing heterotrophic microbial activity in their model (Brouwer et al., 1998), parameters describing NO_2^--N oxidation were poorly identifiable even when slow NO_2^--N oxidation kinetics caused extended tailing in batch respirograms of simultaneous carbon and nitrogen oxidation. Additionally, the model incorrectly assumes NO_2^--N to be the assimilative nitrogen source for NO_2^--N oxidation [inconsistent with Eq. (2)]. The substrate depletion models proposed by Mauret et al. (1996) and Gee et al. (1990) neglect NH_4^+-N incorporation into NH_4^+-N oxidizing biomass. Based on the experimentally determined $f_{S,ns}$ value of 0.084, approximately 3% of the total nitrogen consumed by NH_4^+-N oxidizing bacteria is assimilated and as such cannot be ignored (Chandran and Smets, 2000).

Parameter Identifiability of the Two-Step Model

When NH_4^+-N oxidation kinetics are slower than NO_2^--N oxidation kinetics, the NO_2^--N oxidation profile cannot be differentiated from the overall nitrification profile (Figs. 3 and 5). Therefore, the kinetics of both steps are practically unidentifiable from such a respirogram due to insufficient information pertaining to NO_2^--N to NO_3^--N oxidation. An improvement in the information content of NH_4^+-N oxidation respirograms during dual limitation by NH_4^+-N and NO_2^--N oxidation kinetics is underlined by an increase in the values of $det(F)$ and $\lambda_{min}(F)$ and a decrease in the values of $tr(F^{-1})$ (Table V). Further, as the information content of an NH_4^+-N oxidation respirogram improves, the precision of the kinetic parameters estimated from such a respirogram increases (Table VI). The low values of the standard errors of kinetic parameter estimates obtained from individual respirograms (Table VI) strongly suggest that the higher standard deviations in the kinetic parameter estimates averaged over the duration of this study are due to temporal variation in the culture's biokinetics.

Decreasing NO_2^--N oxidation kinetics also result in a decrease in correlation between the kinetic parameter estimates for NH_4^+-N oxidation and NO_2^--N oxidation (Table IV; Figs. 3–6). The high degree of correlation between μ_{max} and K_S for the two individual steps is typical of parameter estimates for Monod-type functions obtained from batch respirograms and can be substantially reduced by modifying the experimental design used for parameter estimation (Vanrolleghem et al., 1995).

Thus, given an appropriate experimental design and an adequate mathematical description of nitrification kinetics, it should be possible to quantify both steps explicitly without resorting to analytically difficult uncoupling of NH_4^+-N and NO_2^--N oxidation using selective nitrification inhibitors. When NH_4^+-N oxidation limits overall nitrification, we propose injecting NO_2^--N injection close to the point of NH_4^+-N exhaustion to improve practical identifiability of the two-step model parameter estimates, as suggested for a similar scenario (Vanrolleghem et al., 1995).

CONCLUSIONS

Two-step nitrification models are applicable for describing complete NH_4^+-N oxidation profiles only when they contain

Table VI. Precision of two-step model parameter estimates for different rate-limiting scenarios.

		Standard error for parameter			
Case	Rate-limiting oxidation step	$q_{max,ns}$ mg COD / mg NOD h	$K_{S,ns}$ mg NOD L^{-1}	$q_{max,nb}$ mg COD / mg NOD h	$K_{S,nb}$ mg NOD L^{-1}
1	NH_4^+−N to NO_2^-−N	$1.87 \cdot 10^{-3}$	0.076	0.28	0.395
2	NH_4^+−N to NO_2^-−N and NH_2^-−N to NO_3^-−N	$1.12 \cdot 10^{-3}$	0.016	$3.2 \cdot 10^{-3}$	0.0223
3	NH_2^-−N to NO_3^-−N (severely)	$7.41 \cdot 10^{-4}$	0.0116	$5.25 \cdot 10^{-4}$	0.008

adequate kinetic information pertaining to both NH_4^+-N and NO_2^--N oxidation. Dual rate-limitation of overall nitrification by NH_4^+-N and NO_2^--N oxidation kinetics engender maximum precision in the two-step model kinetic parameter estimates compared to rate-limitation by NH_4^+-N oxidation kinetics alone. Under dual limitation, the kinetic parameter estimates obtained from complete NH_4^+-N oxidation respirograms were in good agreement with the estimates obtained from isolated NO_2^--N oxidation assays.

We deeply thank Dr. Peter A. Vanrolleghem, University of Ghent, for sharing his expertise on parameter identifiability with us during the preparation of this manuscript.

NOMENCLATURE

S_{nh}	NH_4^+-N concentration (mg NOD L^{-1})
OU_{ns}	oxygen uptake accompanying NH_4^+-N to NO_2^--N oxidation (mg O_2 L^{-1})
X_{ns}	NH_4^+-N oxidizing biomass concentration (mg COD L^{-1})
$\mu_{max,ns}$	maximum specific-growth rate for NH_4^+-N to NO_2^--N oxidation (h^{-1})
$K_{S,ns}$	half-saturation coefficient for NH_4^+-N to NO_2^--N oxidation (mg NOD L^{-1})
$q_{max,ns}$	maximum specific NH_4^+-N consumption rate (mg NOD mg COD^{-1} h^{-1})
$f_{S,ns}$	biomass-yield coefficient for NH_4^+-N to NO_2^--N oxidation (mg X_{ns} COD produced/mg NH_4^+-NOD oxidized)
S_{no2}	NO_2^--N concentration (mg NOD L^{-1})
OU_{nb}	oxygen uptake accompanying NO_2^--N to NO_3^--N oxidation (mg O_2 L^{-1})
X_{nb}	NO_2^--N oxidizing biomass concentration (mg COD L^{-1})
$\mu_{max,nb}$	maximum specific-growth rate for NO_2^--N to NO_3^--N oxidation (h^{-1})
$K_{S,nb}$	half-saturation coefficient for NO_2^--N to NO_3^--N oxidation (mg NOD L^{-1})
$q_{max,nb}$	maximum specific NO_2^--N consumption rate (mg NOD mg COD^{-1} h^{-1})
$f_{S,nb}$	biomass yield coefficient for NO_2^--N to NO_3^--N oxidation (mg X_{nb} NOD produced/mg NO_2^--NOD oxidized)
k	pseudo-first-order rate coefficient (h^{-1})
F	Fisher information matrix
X	error covariance matrix
AS	activated sludge
df	degrees of freedom
RMS	residual mean square
SE	standard error
N	number of experimental observations
NEC	nitrifying enrichment culture
P	number of parameters
SSE	sum of squared errors (mg^2 L^{-2})
SBR	sequencing batch reactor

Greek Letters

α	probability of incorrectly rejecting the null hypothesis in statistical comparison tests when it is true
β	probability of incorrectly accepting the null hypothesis in statistical comparison tests when it is false. Only applicable when the null hypothesis is not rejected and the parameters being compared are not significantly different.
$\delta\theta$	perturbation in a parameter estimate (θ) normalized with respect to the optimum model prediction value
λ	eigenvalue

References

Brouwer H, Klapwijk A, Keesman KJ. 1998. Identification of activated sludge and wastewater characteristics using respirometric batch-experiments. Wat Res 32:1240–1254.

Chandran K. 1999. Biokinetic characterization of ammonia and nitrite oxidation by a mixed nitrifying culture using extant respirometry. Ph.D. thesis, University of Connecticut, Storrs.

Chandran K, Smets BF. 2000. Single-step nitrification models erroneously describe batch ammonia oxidation profiles when nitrite oxidation becomes rate limiting. Biotechnol Bioeng, 68:396–406.

Dochain D, Vanrolleghem PA, Van Daele M. 1995. Structural identifiability of biokinetic models of activated sludge respiration. Wat Res 29: 2571–2578.

Eaton AD, Clesceri LS, Greenberg AE, editors. 1995. Standard methods for the examination of water and wastewater. Washington, DC: APHA, AWWA and WEF.

Ellis TG, Barbeau DS, Smets BF, Grady CPLJ. 1996. Respirometric technique for determination of extant kinetic parameters describing biodegradation. Water Environ Res. 68:917–926.

Gee CS, Suidan MT, Pfeffer JT. 1990. Modeling of nitrification under substrate-inhibiting conditions. J Environ Eng 116:18–31.

Ginestet P, Audic JM, Urbain V, Block JC. 1998. Estimation of nitrifying bacterial activities by measuring oxygen uptake in the presence of the metabolic inhibitors allylthiourea and azide. Appl Environ Microbiol 64:2266–2268.

Goodwin G. 1987. Identification: Experimental design. In: Singh M, editor. Systems and control encyclopedia. Oxford: Pergamon Press. p 2257–2264.

Grady CPLJ, Daigger GT, Lim HC. 1999. Biological wastewater treatment. New York: Marcel Dekker.

Knowles G, Downing AL, Barrett MJ. 1965. Determination of kinetic constants for nitrifying bacteria in mixed culture with the aid of an electronic computer. J Gen Microbiol 38:263–278.

Ljung L. 1987. System identification—Theory for the user. Englewood Cliffs, NJ: Prentice-Hall.

Mauret M, Paul E, Puech-Costes E, Maurette MT, Baptiste P. 1996. Application of experimental research methodology to the study of nitrification in mixed culture. Wat Sci Tech 34:245–252.

Munack A. 1991. Optimization of sampling. In: Schügerl K, editor. Biotechnology, a multi-volume comprehensive treatise, vol. 4. Measuring, modelling and control. Weinheim: VCH. p 251–264.

Ossenbruggen PJ, Spanjers H, Klapwijk K. 1996. Assessment of a two-step nitrification model for activated sludge. Wat Res 30:939–953.

Ossenbruggen PJ, Spanjers HA, Aspegren H, Klapwijk A. 1991. Designing experiments for model identification of the nitrification process. Wat Sci Tech 24:9–16.

Ott RL. 1993. An introduction to statistical methods and data analysis. Belmont, CA: Duxbury Press.

Prakasam TBS, Loehr RC. 1972. Microbial nitrification and denitrification in concentrated wastes. Wat Res 6:497–509.

Robinson JA. 1985. Determining microbial kinetic parameters using nonlinear regression analysis. In: Marshall KC, editor. Advances in microbial ecology. New York, London: Plenum Press. p 61–114.

Sharma B, Ahlert RC. 1977. Nitrification and nitrogen removal. Wat Res 11:897–925.

Vanrolleghem PA, Vandaele M, Dochain D. 1995. Practical identifiability of a biokinetic model of activated sludge respiration. Wat Res 29: 2561–2570.